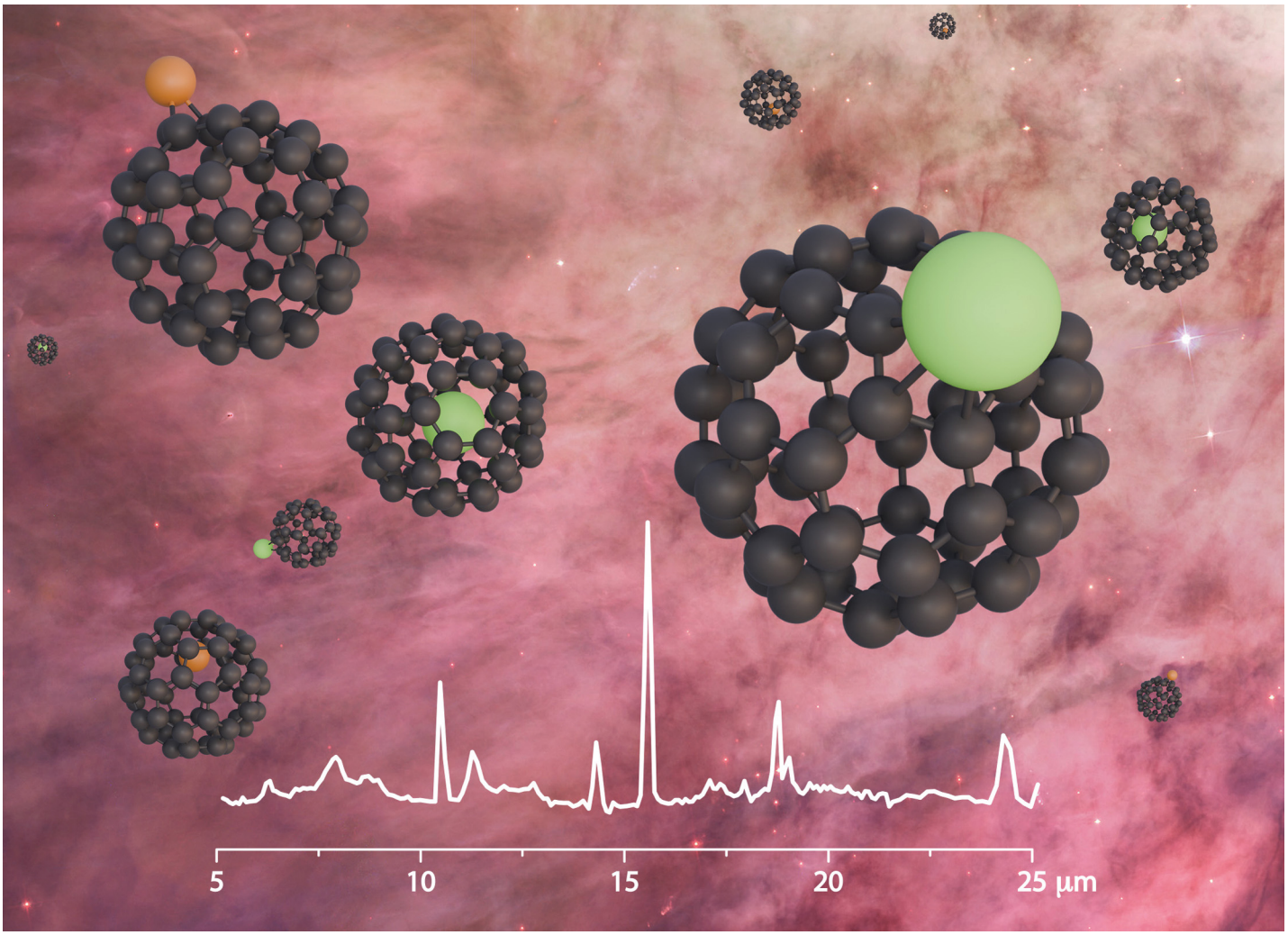

Showcasing research from the group of Prof. Gao-Lei Hou at Xi'an Jiao Tong University, China and Dr Ransel Barzaga at Instituto de Astrofísica de Canarias, Spain

Metallofullerenes as potential candidates for the explanation of astrophysical phenomena

This work discusses the potential relevance of metallofullerenes, either exohedral or endohedral, along with unexplained data or poorly explained astrophysical phenomena, in light of recent advances from both laboratory infrared spectroscopy experiments and quantum chemistry calculations on metallofullerenes from the authors. In particular, the impact of metallofullerenes on understanding the carriers of unidentified infrared emission bands and diffuse interstellar bands was highlighted. This work is expected to gain great attention in the JWST era.

Background image source: NASA

As featured in:

See Ransel Barzaga and Gao-Lei Hou, *Phys. Chem. Chem. Phys.*, 2024, **26**, 13622.

ROYAL SOCIETY OF CHEMISTRY

rsc.li/pccp

Registered charity number: 207890

PCCP Owner Societies

PCCP

ROYAL SOCIETY OF CHEMISTRY

PERSPECTIVE

View Article Online
View Journal | View Issue

Cite this: *Phys. Chem. Chem. Phys.*, 2024, **26**, 13622

Metallofullerenes as potential candidates for the explanation of astrophysical phenomena

Ransel Barzaga †*[ac] and Gao-Lei Hou †*[b]

Detection of complex organic species in space has been one of the biggest challenges of the astrophysical community since the beginning of space exploration, with C_{60}-fullerene representing one of the largest molecules so far detected. The presence of small metal-containing organic molecules, like MgNC or CaCN, in space, promoted the idea that C_{60} may also interact with metals and form metallofullerenes based on the fact that in certain circumstellar and interstellar environments, the ingredients for the formation of metallofullerenes, *i.e.*, metal and fullerenes, are abundant. In this perspective, we summarized the current effort to explore the presence of metallofullerenes in space, which started soon after the discovery of fullerenes about 40 years ago. Several implications of astrophysical phenomena were briefly discussed and shown to be addressable as the possible consequence of metallofullerenes' presence. We highlighted the spectral fingerprints that might be followed to achieve the future detection of cosmic metallofullerenes from a combined effort of laboratory and quantum chemical calculations. These results are expected to gain great importance with the James Webb Space Telescope (JWST), whose capability of unprecedented high sensitivity and high spectral resolution in the far- to mid-infrared range could aid the unequivocal detection of metallofullerenes in space.

Received 12th January 2024,
Accepted 5th March 2024

DOI: 10.1039/d4cp00146j

rsc.li/pccp

1. Introduction

One of the biggest challenges for astrophysics is to detect complex organic species in space. To date, about 300 molecules, composed of different chemical elements, have been detected in a variety of cosmic environments: interstellar/circumstellar medium, protoplanetary disks, and exoplanets, among others.[1,2] The majority of these molecules are carbon-based species, which have been observed in circumstellar and interstellar media.[1,2] Fullerenes, including C_{60}, C_{70}, and C_{60}^+, are the largest carbon-based molecules detected so far in space, for example in hydrogen-rich circumstellar/interstellar environments.[3–6] The presence of C_{60} is deduced from its four infrared emission bands at 7.0, 8.5, 17.4, and 18.9 μm by Cami *et al.* in 2010,[3] which raises a new era for cosmic fullerene chemistry. Fullerene-based molecules have been highlighted as potential candidates to explain several astrophysical phenomena, for instance, the unidentified infrared emission (UIE) bands, the UV-bump or the diffuse interstellar bands (DIBs).[1,7,8] Both UIE bands and DIBs include multiple spectral signals that have not yet been assigned to any molecular species,[9,10] driving the effort to search for new candidates.

Interestingly, metal-containing organic molecules (with metals such as Mg, Na, Al, K, Fe, and Ca) have been detected in the circumstellar environments of evolved stars, where C_{60} has also been confirmed to exist.[11–13] Undeniable examples of these metal–organic molecules include MgNC, NaCN, CaNC, *etc.*, implying that organic species and metals can coexist in the circumstellar environment and form more complex metal–organic species.[2,14,15] In addition, the circumstellar medium of evolved stars is rich in terms of metal abundances,[16,17] making it plausible that in a medium which is rich in both fullerenes and metals, metallofullerenes can also form and exist.

In fact, metallofullerenes have already been employed to explain several astrophysical observations, but mainly speculatively until recently.[18,19] In this perspective, we focus on the current efforts to understand the relevance of metallofullerenes as astrophysical species. The comparison of the infrared emission spectra from astrophysical objects against laboratory measurements and theoretical simulations is overviewed towards the future detection of cosmic metallofullerenes, and their infrared spectral fingerprints are highlighted as important signatures to confirm or refute their presence. The astrophysical

[a] *Instituto de Astrofísica de Canarias, C/Via Láctea s/n, E-38205 La Laguna, Spain. E-mail: rbarzaga@iac.es*
[b] *MOE Key Laboratory for Non-Equilibrium Synthesis and Modulation of Condensed Matter, School of Physics, Xian Jiaotong University, Xian, 710049 Shaanxi, People's Republic of China. E-mail: gaolei.hou@xjtu.edu.cn*
[c] *Departamento de Astrofísica, Universidad de La Laguna (ULL), E-38206 La Laguna, Spain*
† Ransel Barzagaa and Gao-Lei Hou have contributed equally to this work.

implications of metallofullerenes are discussed, permitting their potential significance in the James Webb Space Telescope (JWST) era.

2. Early intends of metallofullerenes search

Already after the discovery by Kroto, Smalley, Curl, and coworkers in 1985,[20] the remarkable thermal and radiative stability of C_{60}-fullerene led Kroto to speculate that fullerene derivatives could be present as potential complex species in space.[21] Later on, experimental evidence of endohedral and exohedral metallofullerenes showed the propensity of alkaline and alkaline earth metals to complex with fullerenes.[22–24] These findings motivated the prediction of electronic transition energies of metallofulerenes, either exohedral or endohedral, through a first order approximation. Based on an electron hopping model (see Fig. 1), Kroto and Jura described the charge-transfer (CT) mechanism of the metallofullerene taking place during photoprocessing.[25] Accordingly, the charge transfer would produce specific electronic bands in the ultraviolet spectral regime for metals such as Na, K, Ca, and Al, while manifesting in the mid-infrared spectral region for metals like Fe. This prediction assumes that the CT transitions of metallofullerenes solely depend on the ionization potentials of C_{60} and metals and neglects the effect of the exact geometries. Hence, these CT bands are virtually the same for both exohedral and endohedral metallofullerenes according to the assumption. Although the assumption is vague and thus the estimated band positions are not accurate, they are still meaningful for providing a first model for the possible track of their electronic transitions in space as experimentally measuring these transitions is of significant challenge.[7] Nonetheless, Kroto and Jura are among the first to speculate about metal-containing species in space, beyond those already known at that time, *e.g.* MgS or $(Mg,Fe)_2SiO_4$ (olivine), among other minerals.[26–32]

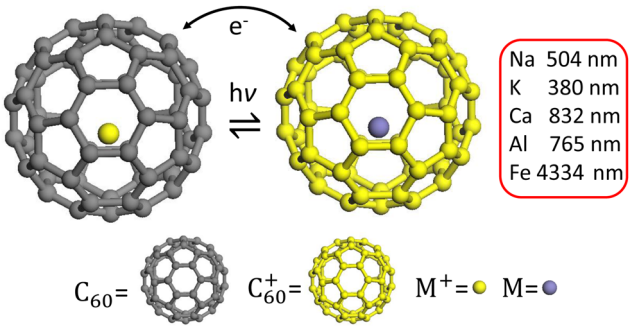

Fig. 1 Schematic of the electron hopping assumption by Kroto and Jura to describe the electronic transition of a metallofullerene following a first order approximation. Note that here we employ endohedral metallofullerenes for demonstration purpose. Different colours denote the charged and neutral states of the carbon cage and metal, respectively. The red square highlights the values of the CT transition energies in wavelength (ref. 25).

However, the above-mentioned speculations by Kroto and Jura are not seriously considered until 2010, when C_{60} and C_{70} fullerenes were confirmed in circumstellar and interstellar environments.[3] The detection of fullerenes has been achieved mostly in cosmic objects rich in hydrogen, such as planetary nebulae, R Coronea Borealis stars, protoplanetary nebulae, and in the interstellar medium or even in oxygen-rich environments.[4,5,33–35] Thereafter, the interest in metallofullerenes reemerges because both metals and fullerenes are abundant enough to possibly form new metal–organic species.

3. Metallofullerenes in the laboratory

One of the most intriguing astrophysical puzzles is the enrichment of carbonaceous dust with other elements because the dust is ejected into the interstellar medium, affecting the interstellar chemistry and subsequent stellar evolution.[36,37] Experimental investigation showed that endohedral metallofullerenes might be relevant to the evolution of carbon dust in the interstellar medium. Dunk *et al.*[38] experimentally explored carbon condensation, one possible mechanism of fullerene formation,[39,40] and the interaction with Na under highly energetic conditions. They found that for a metallofullerene, like Na@C_{60}, to be astrochemically viable, the endohedral metal atom must be an element that could readily incorporate into the fullerene cage. Furthermore, they also explored the formation of metallofullerenes under astrochemically relevant conditions with oxygen and hydrogen-rich environments in the experiment.

The experimental procedure includes ablating a Na-doped carbon rod to produce plasma in a He flow and the nucleation of the Na atom inside the carbon cage to form a metallofullerene. An entire family of endohedral metallofullerenes has been obtained using this approach, with Na@C_{60} being the most

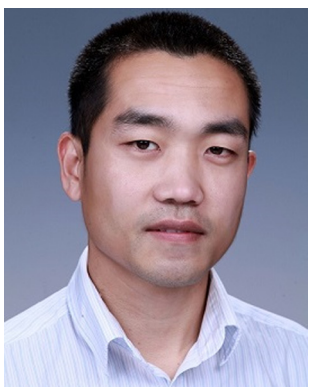

Gao-Lei Hou

Gou-Lei Hou is currently a professor at Xi'an Jiaotong University (China). He obtained his BS and PhD degrees from the University of Electronic Science and Technology of China (2009) and the Institute of Chemistry, Chinese Academy of Sciences (2014), respectively. He underwent professional postdoctoral training with partial teaching duty at Pacific Northwest National Laboratory (USA), ETH Zurich (Switzerland), and KU Leuven (Belgium) from 2014 to 2021. With backgrounds in chemical physics, molecular physics, and quantum chemical computations, he is now working at the interfaces of physics, chemistry, and astronomy, with current research interest in laboratory astrophysics and astrochemistry, catalytic energy conversion and transformation, and cluster-based functional materials and prototype devices.

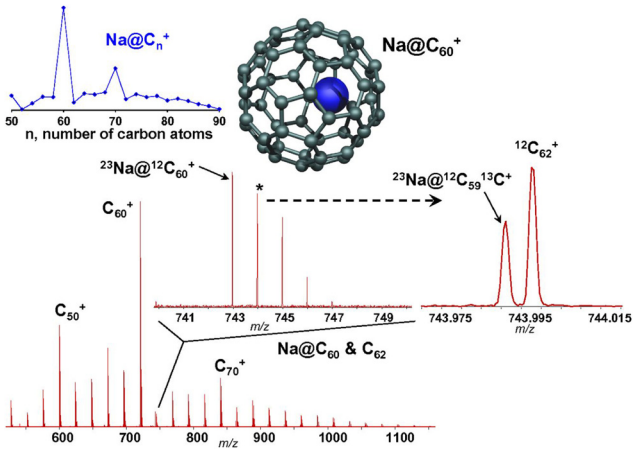

Fig. 2 Mass spectrometry of clusters formed during Na-doped carbon condensation. The Na@C_{60} signal is clearly resolved from C_{62}. The inset shows the relative abundances of Na@C_n species. Figure reprinted with permission from ref. 38. Copyright 2013 National Academy of Sciences.

abundant among Na@C_{2n} clusters (Fig. 2). In fact, the distribution of Na@C_{2n} clusters shown in Fig. 2 indicates that similarity may exist in the formation mechanism of metallofullerenes, which has been considered as a metal-containing carbon nucleation process.[39,40] The formation of C_{60} during carbon nucleation kinetically hinders the production of other fullerenes, making it predominant with respect to smaller and larger fullerenes. The inset in Fig. 2 shows a similar trend with a predominant abundance of Na@C_{60} over other Na@C_n clusters, implying the structural resemblance between C_{60} and Na@C_{60}. Also in Fig. 2, it can be seen that the abundance of Na@C_{60} is lower than the empty carbon cages (*e.g.* C_{70}, C_{60}, and C_{50}). Relative abundance of Na@C_{60} decreases when flows of H and O are added to simulate the hydrogen and oxygen-rich circumstellar/interstellar environments, showing that in cosmic environments, it could be possible to form metallofullerenes.[38]

Endohedral metallofullerenes could also be obtained using an electric arc plasma discharge technique of a metal-doped graphite, which might be slightly less harsh compared to laser ablation.[41] Using this technique, Dunk *et al.* produced a series of endohedral metallofullerenes (M@C_{2n}) with different metals, including alkaline metals, alkaline earth metals, and transition metals (Fig. 3). A striking trend has been observed regarding the abundance distribution of M@C_{2n}, which depends on the charge and chemical nature of the metals, as well as the fullerene size. They found that charge transfer (metal to carbon cage) and ionic radii are the main factors driving the formation of M@C_{2n}. Such a finding is somewhat in accordance with the earlier proposal by Kroto and Jura that the charge transfer is important to understand the cosmic relevance of metallofullerenes.

Fig. 3 shows that not all metal elements could form endohedral metallofullerenes using the electric arc plasma discharge technique, for example, endohedral metallofullerenes have not been found for several cosmically abundant elements, such as Li, Mg, and Fe. However, other techniques, for instance, the ion implantation technique followed by light oxidation and stabilization with the corresponding counterion may be utilized to produce endohedral fullerenes for those metals not obtainable by using the electric arc plasma discharge technique.[43–45] In this synthetic approach, metallofullerenes are accompanied by a counterion to stabilize the charge balance, and it is useful to provide laboratory samples for the spectral analysis of these species, although this formation route seems clearly not possible under the astrophysical conditions.[38]

In order to estimate the abundance of fullerenes or metallofullerenes in cosmic environments, it is essential to obtain the laboratory spectroscopic property, for instance in the infrared spectra, to compare with astronomical observations. Estimation of the abundance involves the information about the molar extinction coefficient (ε) and the integrated molar absorptivity (ψ) of the infrared bands.[46–48] In this sense, García-Hernández *et al.*[42] studied the mid- and far-infrared property of highly purified $[Li@C_{60}]^+PF_6^-$ salt and obtained the ε and ψ values. They found that $[Li@C_{60}]^+PF_6^-$ can emit in a similar mid-infrared spectral region as C_{60}, even with several overlapping infrared bands (Table 1).

Furthermore, far-infrared spectra demonstrate the dynamics of the lithium atom inside the carbon cage of $[Li@C_{60}]^+$, and

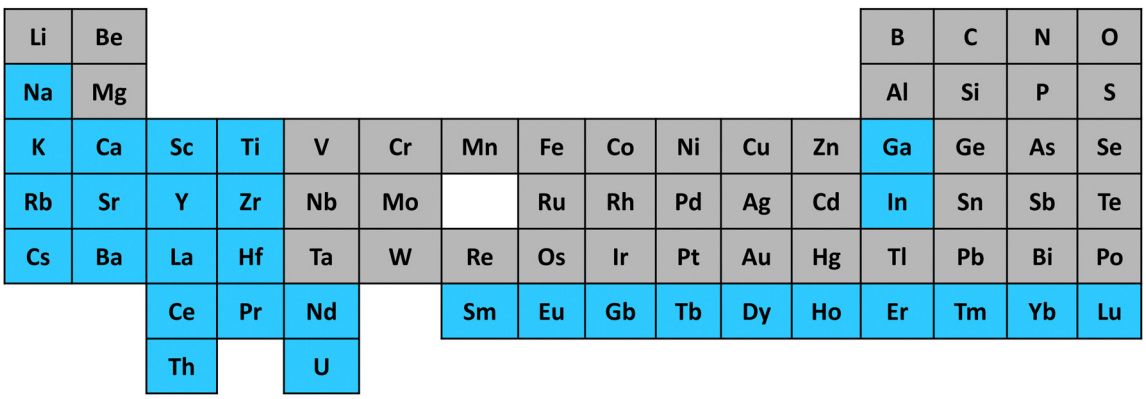

Fig. 3 Specific elements for which endohedral metallofullerenes are synthesized using the electric arc plasma discharge technique. Metallofullerenes are obtained only for the chemical elements filled in light blue, while the opposite occurs for those in gray. Extracted from ref. 41.

Table 1 Molar extinction coefficient (ε) and integrated molar absorptivity (ψ) of $[Li@C_{60}]PF_6$ *vs.* C_{60}. Extracted from ref. 42

Wavenumber (cm^{-1})	Wavelength[a] (μm)	$[Li@C_{60}]PF_6$ (ε) (L mol^{-1} cm^{-1})	C_{60} (ε) (L mol^{-1} cm^{-1})	$[Li@C_{60}]PF_6$ (ψ) (km mol^{-1})	C_{60} (ψ) (km mol^{-1})
1421	7.04	106	63	10.8	10.4
1180	8.47	145	61	8.1	9.4
960	10.42	53		2.0	
837	11.95	1103		234.8	
578	17.30	166	101	3.7	16.2
560	17.86	393		9.2	
554	18.05	216		23.3	
530	18.87	428	234	24.2	30.2

[a] Astrophysical community uses the wavelength notation.

two far-infrared bands at 152 and 164 cm^{-1} are assigned to the movement of lithium inside the C_{60} cage, with the aid of theoretical calculations.[49] It is worthwhile to note that the band at 76 cm^{-1} is accompanied by a weak shoulder at 64 cm^{-1} that is provoked by the interaction between $[Li@C_{60}]^+$ and its counter-ion PF_6^-.[42,49] These studies suggested that endohedral metallofullerenes are likely to be more easily detected in the far-infrared regime of cosmic objects because C_{60} lacks far-infrared bands, eliminating the potential band overlapping (Fig. 4).[49]

In addition, García-Hernández *et al.* also studied the thermal effect on the infrared fingerprint of $[Li@C_{60}]^+PF_6^-$ because C_{60}-fullerene has been detected under different thermal conditions of the cosmic environments in space.[5,33,34] They found that the infrared bands of fullerenes shift as a function of temperature,[50] suggesting that endohedral metallofullerenes might have similar behavior. The derived set of semiemperical equations for predicting the temperature-dependent frequencies of the infrared bands of $[Li@C_{60}]^+PF_6^-$ is summarized as mentioned below. It is found that the bands coincident between C_{60} and $[Li@C_{60}]^+PF_6^-$ (Table 1) almost fulfill the same equations.

$$\nu_4 = -0.0176T + 1426.6$$

$$\nu_3 = -0.0087T + 1182.1$$

$$\nu_2 = -0.0059T + 579.6$$

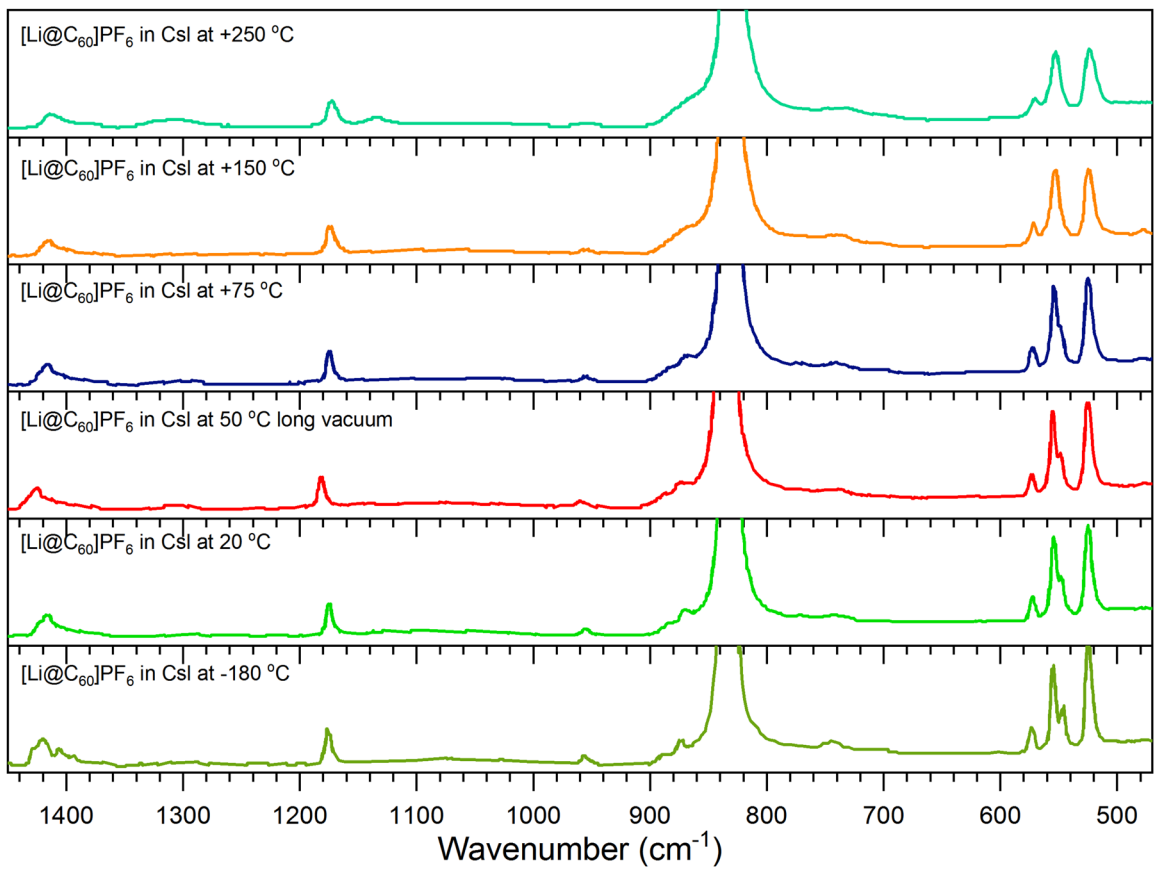

Fig. 4 Mid-infrared spectra of $[Li@C_{60}]PF_6$ recorded at different temperatures. The range of temperature is denoted in each graphic. Figure digitized from ref. 42.

In general, the increment of the temperature provokes a downshift of the mid-infrared bands, although the band at 530 cm^{-1} for both C_{60} and $[Li@C_{60}]^+PF_6^-$ is thermally insensitive. This interesting work also implies that endohedral metallofullerenes preserve a similar high thermal stability as C_{60}, allowing them to survive the highly energetic conditions of cosmic environments.

Recently, Hou *et al.* have developed a state-of-the-art experimental protocol to synthesize and measure the laboratory infrared spectroscopy of gas-phase fullerene–metal complexes, more specifically the singly charged exohedral metallofullerenes, *via* dual laser ablation and messenger-tagged infrared multiple photon dissociation (IRMPD) spectroscopy.[19,51–53] Fig. 5 presents the mass distributions of the synthesized $C_{60}Fe^+$ complexes and the laboratory IRMPD spectrum of Ar-tagged $C_{60}Fe^+$, as well as the simulated infrared spectrum of $C_{60}Fe^+$ obtained from quantum chemical calculations. It can be seen from Fig. 5b that apart from the four main features that coincide with the neutral C_{60} bands, as indicated by the vertical red dotted lines, many more vibrational bands appear. A comparison of Fig. 5c and b shows that the theoretical calculations can reproduce essentially all observed infrared features, except that certain band intensities show a slight discrepancy. This is common when comparing the intensity from quantum chemical calculations with IRMPD experiments due to the multiple-photon excitation effect,[19,51,54] and similar results have been obtained for $C_{60}Rh^+$, $C_{60}V^+$ and its water absorbed complexes.[19,51–53,55] These findings lend confidence that quantum chemical calculations can reliably predict the infrared spectra of C_{60} complexes with cosmically abundant metals, such as Li, Na, K, Mg, Ca, and Al.[8] Theoretical calculations show that all these exohedral metallofullerenes have similar infrared spectral patterns as that of $C_{60}Fe^+$ (see Fig. A3 in ref. 19). Detailed vibrational analysis suggests that most of the infrared features come from the motions of the C_{60} cage, perturbed by the attaching metal atoms. Hence, they concluded that the laboratory spectrum of $C_{60}Fe^+$ can be considered as a model for various cationic exohedral metallofullerenes to investigate the potential spectral impact of the presence of exohedral metallofullerenes in space.

They further compared the laboratory infrared spectrum of the $C_{60}Fe^+$ complex with the Spitzer infrared spectra of several fullerene-rich planetary nebulae (PNe), and found a strong positive linear cross-correlation. Interestingly, they found that the co-existence of different exohedral fullerene–metal complexes in the same object could slightly modify the band positions and intensities, which may explain the shoulders and asymmetric band profiles observed in the 17–20 μm region (see in Fig. 6), and regulate the ratios of the four C_{60} bands by the varied spectral intensities for different metals, thus potentially resolving the long-standing issue of the wide-spread observational intensity ratios of the four C_{60} bands.[56,57] In addition, they found that the infrared spectra of fullerene–metal complexes may also explain several other yet unidentified features.[19,58]

Fig. 6 shows the temperature and abundance required for each species to replicate the observed emission spectra of the

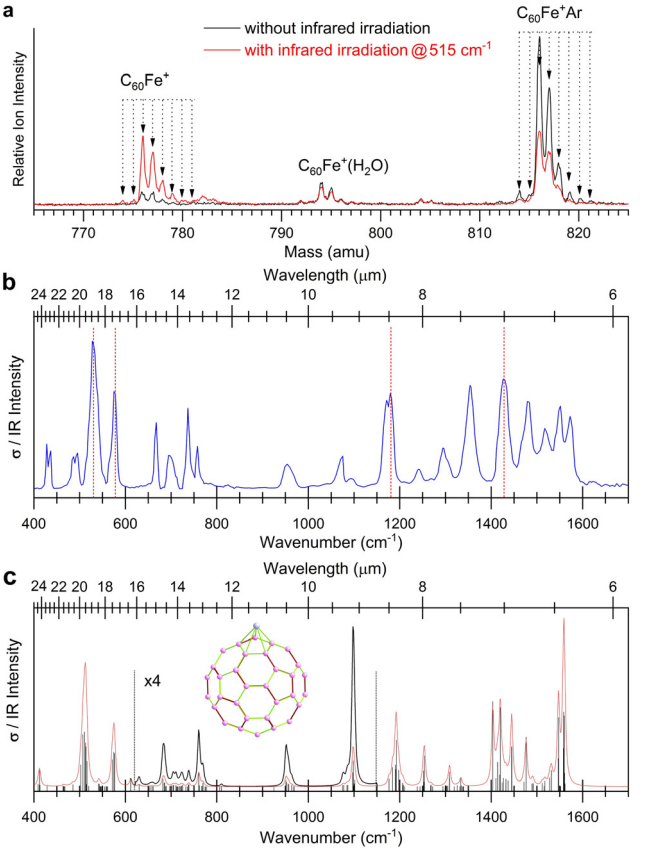

Fig. 5 Laboratory synthesis and infrared spectroscopy of $C_{60}Fe^+$. (a) Mass distributions of $C_{60}Fe^+$ and its Ar-tagged complexes synthesized using a dual-laser ablation source, with (red) and without (black) the infrared irradiation at 515 cm^{-1}. (b) IRMPD spectrum of Ar-tagged $C_{60}Fe^+$. The four neutral C_{60} bands are indicated using vertical red dotted lines. (c) Theoretically simulated spectrum of $C_{60}Fe^+$ at the BPW91/6-31G(d) level (red curve) with its calculated structure shown as the inset. The calculated intensities are plotted with sticks and convolved using Lorentzian line shapes of 6 cm^{-1} full width at half maximum. The convolved spectrum is enlarged by a factor of four between 650 and 1150 cm^{-1} (black curve). Figure reprinted with permission of ref. 19. Copyright 2023 American Astronomical Society.

four fullerene-rich PNe, based on thermal emission models that treat the fullerene–metal complexes as a microcanonical ensemble. They found that about 2.6–7.7× 10^{-8} solar mass ($M_\odot$) of pure C_{60} is required to reproduce the four main emission bands. While for $C_{60}Fe^+$, about 0.69–2.1 × 10^{-7} $M_\odot$ of $C_{60}Fe^+$ or 1.9–6.1% of the available carbon with excitation temperatures above 400 K can give an equally good fit, in addition to the fact that they could also account for some additional emission features. Since both C_{60} and $C_{60}Fe$ have low ionization potentials, their ionized form could be favored, although it would be challenging to accurately estimate the fractions considering the complicated charge balance, involving competition among ionization, electron attachment, and recombination events as well as the lack of parameters associated with those processes.

Based on the high cross-correlation coefficients and good fits of the thermal emission model, Hou *et al.*[19] proposed that

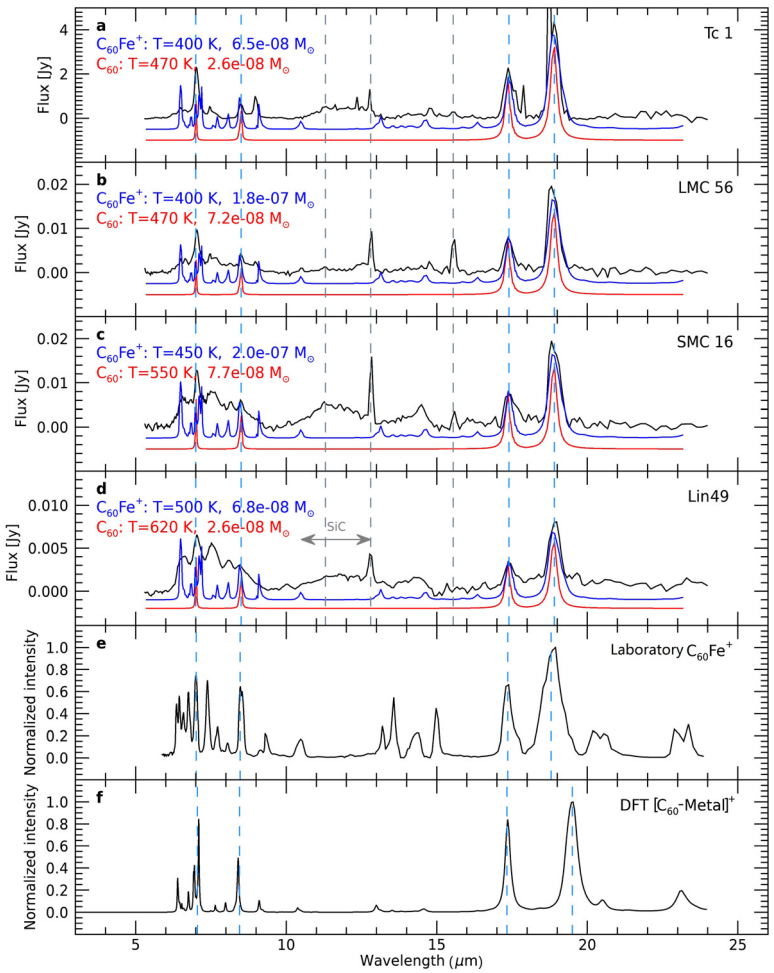

Fig. 6 Comparison between the Spitzer infrared spectra of four fullerene-rich PNe (black) and the thermal emission model for C_{60} (red) and $C_{60}Fe^+$ (blue). (a) Tc 1, (b) LMC 56, (c) SMC 16, and (d) Lin49. The excitation temperatures and mass derived from the thermal emission models based on a microcanonical ensemble are indicated at the left in each panel. (e) Laboratory infrared spectrum of $C_{60}Fe^+$. (f) Summed theoretical spectrum of cationic exohedral fullerene–metal complexes. The blue and gray dashed lines indicate the four observational or calculated C_{60} bands, and strong atomic emission lines, respectively. Figure reprinted with permission of ref. 19. Copyright 2023 American Astronomical Society.

gaseous ionized fullerene–metal complexes are potentially promising candidates for explaining the infrared emission spectra of the fullerene-rich PNe in addition to neutral C_{60}, opening the door for a real consideration of Kroto's hypothesis over 30 years ago. Moreover, they found that the complexation of metals with fullerenes could lead to a far richer spectrum in the visible and near-infrared spectral range than fullerenes themselves, due to the charge transfer from the metal to the carbon cage, making them potential candidates for diffuse interstellar bands (DIBs).[59] The recent findings performed by Campbell *et al.*,[60,61] about the synthesis of C_{60}^+ ions tagged with helium and its UV-visible spectrum measurement, show experimental possibility that would support the speculations by Hou *et al.*[19] about the charge transfer process of metallofullerenes and their contribution to the visible regime. Metals are widely known to be active catalysts for the synthetic production of various carbon nanostructures, including carbon cages under oxygen- and hydrogen-rich conditions as found by Dunk *et al.*[38,41] Then, one may speculate from the study of Hou *et al.*[19] that metal atoms and their ions might also play a catalytic role in fullerene formation in space, as metallofullerenes, if present, could be considered as byproducts of this catalytic process. Further consideration of the role of metals in cosmic chemical transformations could lead to a breakthrough in our understanding of cosmic carbon chemistry. Seemingly, the challenges in detecting metallofullerenes are quite similar to those once faced by C_{60}^+.

Besides infrared emission, near-infrared and UV-visible were essential in order to unequivocally assign C_{60}^+ as one of the carriers of more than 600 DIBs observed by astronomers. In this sense, the recently reported electronic transitions in endohedral fullerenes, like $He@C_{60}^+$, $H_2O@C_{60}^+$ and $D_2O@C_{60}^+$, using laboratory techniques for their synthesis and spectra measurement, exemplify the strong efforts performed in order to understand the astrophysical observations through the comparison with laboratory data.[62,63] Such efforts could also improve the search of metallofullerenes, which present structural resemblances with these species. Thus, carrying out similar laboratory studies will

move forward to the final detection of metallofullerenes under the astrophysical conditions.

4. Metallofullerenes by quantum chemical calculations

Undoubtedly, the detection of fullerene species (C_{60}) in diverse cosmic environments has raised the possibility that fullerene derivatives, for instance metallofullerenes, might be ubiquitous in space,[8,64] as discussed already above. The possible detection of a molecular species in space requires at least laboratory data that can match with astronomical observations. However, such laboratory efforts have proven to be tremendously challenging, as exemplified by verifying C_{60}^+ as a carrier of DIBs.[7] In this regard, quantum chemical calculations, to some extent, provide a realistic approach to predict both the physical and chemical properties of fullerenes and their derivatives, in particular when there is no laboratory work available. The calculations can be employed to compare and potentially explain certain astrophysical observations. Furthermore, quantum chemical calculations can be combined with astrophysical modelling of the circumstellar/interstellar medium, in order to include more realistic thermal and radiative processes occurring in space. As a result, a more accurate prediction of the species' abundances in space can be achieved, thus, their implications on the infrared spectra can be accounted.

4.1. Metallofullerenes and the C_{60} 17.4/18.9 μm band ratio problem

The C_{60} 17.4/18.9 μm or 578/530 cm^{-1} band ratio problem is an anomaly noted in several previous publications.[56,57] Typically, the C_{60} 17.4/18.9 μm band ratio displays values between 0.41 and 0.79 according to both experimental and theoretical data.[65,66] However, Brieva *et al.* found that in fullerene-rich planetary nebulae, this ratio can reach a value of 1.2, which cannot be explained either by the thermal excitation model or by the fluorescence mechanism.[56] Alternatively, they proposed that if other species that can emit at the same wavelengths as C_{60} and contribute to the observational band intensity, then the problem may be resolved.

Recently, Barzaga *et al.* have carried out quantum chemical calculations on twenty-eight charged and neutral endo- and exohedral metallofullerenes, aming to understand the infrared emission spectra of these species.[18] They found that both endohedral and exohedral metallofullerenes, either neutral or charged, could (i) significantly contribute to the four infrared bands normally attributed to neutral C_{60} in fullerene-rich planetary nebulae and (ii) offer an explanation for the C_{60} 17.4/18.9 μm band ratio problem, similar to the proposal of Hou *et al.*[19] They noted from quantum chemical calculations that different metallofullerenes have infrared bands close or similar to neutral C_{60} (see Fig. 1–4 in ref. 18), and metallofullerenes may affect the 17.4/18.9 μm band ratio, especially the neutral ones. Neutral endo(exo)hedral metallofullerenes ([M@C_{60}] and [M–C_{60}]) produce an inversion of the 17.4/18.9 μm band ratio,

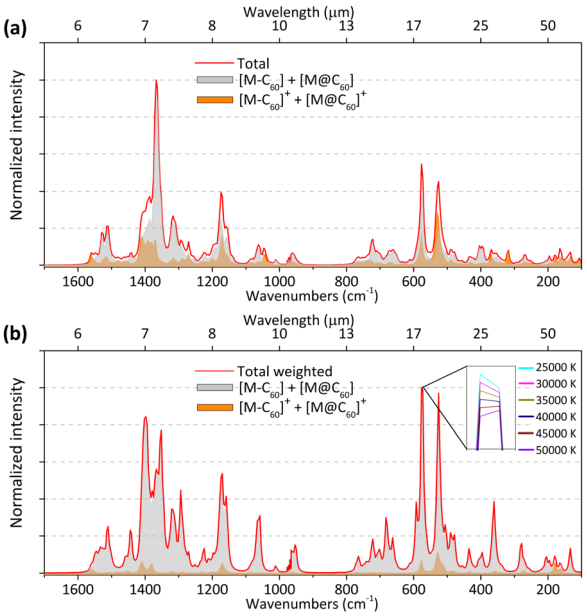

Fig. 7 Infrared spectra of metallofullerenes obtained from the combination of all the species. (a) Total spectrum obtained purely from quantum chemical calculations. (b) Total weighted spectra from quantum chemical simulations under the assumption of astrophysical conditions. The inset shows the dependence on the effective temperature of the central star in the planetary nebulae, against the infrared intensity of the weighted spectra. Figure reprinted with permission of ref. 18. Copyright 2023 American Astronomical Society.

with values for exo- and endo-hedral metallofullerenes of 1.89 and 2.55, respectively.

However, Barzaga *et al.*[18] demonstrated that quantum chemical calculations may bias the prediction of the 17.4/18.9 μm band ratio. Under the assumption of astrophysical metal abundances,[16,17] ionization processes, and possible formation reactions of metallofullerenes, they constructed the infrared spectra that may describe more accurately the effect of cosmic environments (Fig. 7). Accordingly, the interpretation of the simulated and pure quantum-chemical spectra is drastically different in terms of infrared intensities. Consequently, the 17.4/18.9 μm band ratio shown in Fig. 7b exhibits a value of 1.03.

The infrared intensities depend significantly on the level of metal ion production and metal abundances in each cosmic environment, for example planetary nebulae and R Coronae Borealis stars.[4,5,33,34] The trend shown in Fig. 7 shows that neutral metallofullerenes have higher contribution to the infrared spectra (gray shaded area) due to the larger abundances of metals, against ions, in these environments. In general, the simulated spectra suggest that metal abundance is more relevant than other properties of the cosmic environments.

The astrophysical objects herein are planetary nebulae and R Coronae Borealis stars, which are fullerene-rich objects consisting of a central star surrounded by a dust ring (envelope).[67,68] The central star's temperature or effective temperature (T_{eff}) can vary according to the astrophysical object, ranging from ~30 000 to 50 000 K for fulleren-rich planetary

nebulae[69] and around 19 500 K for the hottest R Coronae Borealis star.[5] An inset in Fig. 7 displays the negligible change in the infrared intensity as the temperature increases on the central star of the planetary nebulae, which is likely due to the large metal abundances of Fe and Mg. These two metals present abundances below oxygen, which is a more abundant element, but in only one order of magnitude according to nucleosynthesis model predictions performed by Karakas *et al.*[17] (mass fraction O $\simeq 10^{-3}$; Fe and Mg $\simeq 10^{-4}$). Thus, despite that the formation of metallofullerenes could be limited by the presence of oxygen, Fe and Mg should be the ones which react more with C_{60}. In fact, the above mentioned experiments performed by Drunk *et al.* about the formation of endofullerenes in oxygen and hydrogen-rich environments indicate that even under such conditions, metalloendofullerenes can form.[38] The concept of employing quantum-chemical calculations and astrophysical quantities to simulate the infrared spectra is further extended by Barzaga *et al.*[18] using an ionization probability of neutral metallofullerenes combining with a modification of the coefficients in the following chemical reactions:

$$M + C_{60} \rightarrow a[M@C_{60}] \text{ or } b[M{-}C_{60}]$$

$$M^+ + C_{60} \rightarrow a[M@C_{60}]^+ \text{ or } b[M{-}C_{60}]^+$$

$$[M@C_{60}] \xrightarrow{h\nu} [M@C_{60}]^+$$

$$[M{-}C_{60}] \xrightarrow{h\nu} [M{-}C_{60}]^+$$

where the coefficients a and b in the first two chemical reactions manipulate the endo- to exo-hedral metallofullerene concentration, while the above photoionization reactions affect the overall production of charged metallofullerenes at the expense of the neutral ones. As a result, different correlation curves are obtained using the 17.4/18.9 μm band ratio as a function of the ionization level of neutral metallofullerenes (see Fig. 8).

The result of Barzaga *et al.*[18] lies in the good agreement between the curves in Fig. 8 and the observed 17.4/18.9 μm band ratios in different cosmic environments. The predicted values for the planetary nebulae range from ~0.7 to 1.2, which agree reasonably well with those reported for galactic and extragalactic fullerene-rich planetary nebulae ranging from ~0.2 to 1.2.[33,56] In contrast, the match is quite exceptional for planetary nebulae of the Large Magellanic Cloud (LMC), for which 17.4/18.9 μm band ratios have been reported in ranging from ~0.7 to 1.2[33] (see LMC48 and LMC99 in Fig. 8).

Interestingly, the consistency of the quantum-chemical-simulation approach is proved by the explanation of the striking 17.4/18.9 μm band ratio observed for R Coronae Borealis stars, for which the values reported are ~1.4 and 2.3 for DYCen and V845Cen, respectively.[5,18] The predicted values for these two astrophysical objects vary from ~1.1 to 2.0, which agree very well for DYCen observation, although for V845Cen, these values deviate with respect to the observation (see Fig. 8).

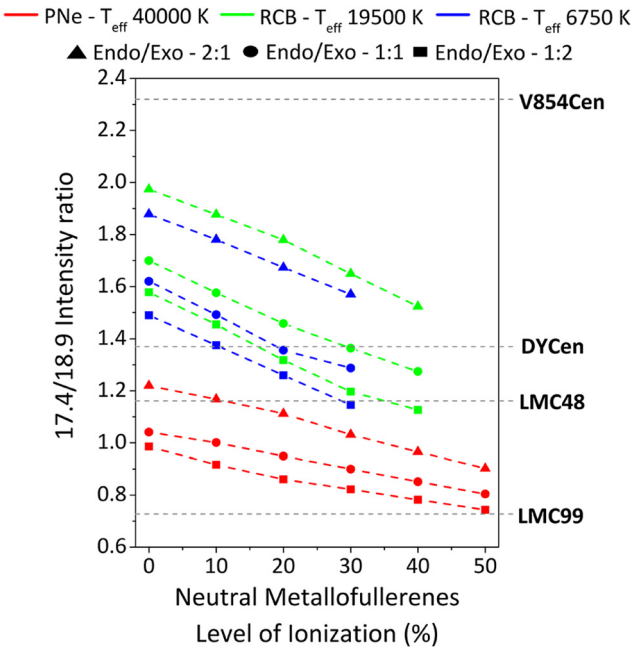

Fig. 8 The 17.4/18.9 μm band ratio as a function of the ionization level of neutral metallofullerenes. Colour is used to identify each curve corresponding to different cosmic environments, which have been sorted according to the effective temperature: Planetary nebulae – PNe (red), Cold R Coronae Borealis – RCB star (blue) and Hot R Coronae Borealis – RCB star (green). In addition, symbols on the curves denote the concentration of the different exo-/endo-hedral metallofullerenes. The horizontal dashed lines indicate the 17.4/18.9 μm band ratio observed in two fullerene-rich PNe (LMC48, LMC99[33]) and two RCB stars (DYCen,[5] V845Cen[18]). Figure reprinted with permission of ref. 18. Copyright 2023 American Astronomical Society.

Nevertheless, the deviation in the case of V845Cen is attributed to an important contribution of carbon aromatic species in this object.[5] The combined method of quantum-chemical calculations and astrophysical quantities by Barzaga *et al.*[18] provides an explanation for the fundamental problem of the large range of 17.4–18.9 μm band ratios observed in different fullerene-rich astrophysical objects. Furthermore, Barzaga *et al.* demonstrate that using the predicted 17.4/18.9 μm band ratios is able to reproduce, at least, this region on the emission spectra of some R Coronae Borealis stars (see Fig. 9).[70]

4.2. Reliable scaling factors

The quantum-chemical modelling of metallofullerenes in cosmic environments requires an accurate comparison of laboratory and observational infrared spectra. Nevertheless, infrared frequencies obtained from quantum chemical calculations may deviate from the laboratory data, and the deviation may depend on the quantum-chemical methods, in particular for density functional theory based calculations. To possibly tackle this problem, scaling factors could be developed to make the calculated harmonic frequencies closely resemble the laboratory data. In this regard, Xu *et al.* recently compiled a VibFullerene database that includes all the so far experimentally measured infrared frequencies of fullerene-related species,

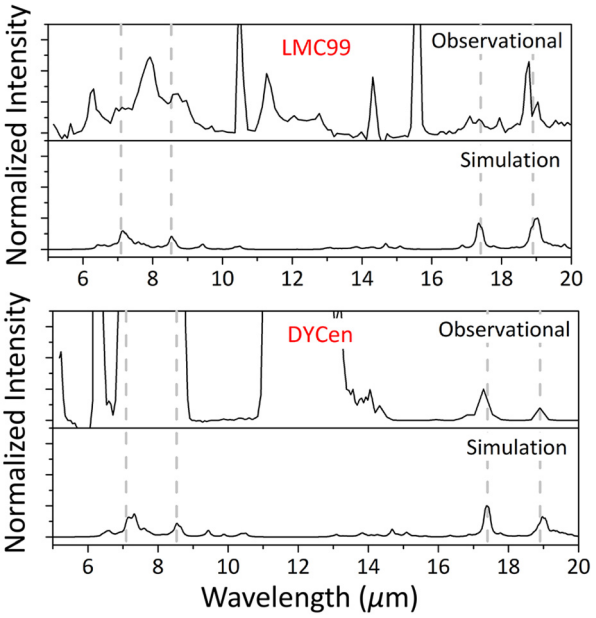

Fig. 9 Comparison of the continuum-subtracted Spitzer Space Telescope (top) and representative metallofullerenes simulated IR spectra (bottom) for two fullerene-rich objects showing very different C_{60} 17.4/18.9 μm band ratios and chemical abundances: the PN LMC 99 and the RCB star DY Cen. The guidelines show the features of pristine C_{60} at 7.09, 8.53, 17.34, and 18.91 μm, according to Barzaga *et al.*[18] The intensity has been normalized according to the 17.4/18.9 μm band ratio under the assumption that metallofullerenes are the only emitters causing the 17.4/18.9 μm anomaly in the spectra; *i.e.*, the more intense feature of the 17.4/18.9 μm pair has been used to establish the reference for normalization. Figure has been reprinted with permission of ref. 70. Copyright 2023 American Astronomical Society.

including C_{60}, C_{70}, C_{60}^{+}, $C_{60}O^{+}$, $C_{60}OH^{+}$, $C_{60}H^{+}$, and $C_{70}H^{+}$, with totally 92 vibrational frequencies.[71] They carried out a systematic theoretical study on these species using several popular density functional theory methods. Following a least-square fitting procedure by minimizing the root mean square error (RMSE), they derived a set of range-specific scaling factors for vibrational frequencies (Table 1). They verified the reliability of the fitted factors by comparing the scaled theoretical and experimental infrared spectra of the $C_{60}V^{+}$ complex and found good agreement, illustrating the usefulness of the scaling factors in predicting the infrared property of metallofullerenes. Accordingly, they noted that the functionals with higher Hartree–Fock (HF) components tend to overestimate the calculated harmonic frequencies more, necessitating smaller scaling factors. Overall, it seems that the functionals with low-HF components exhibit smaller RMSE and median error values, showing slightly better performance (Table 2).

From the systematic study, they suggested that the generalized gradient approximations (GGAs), *i.e.*, BP86 and BPW91, offer a good balance between the accuracy and computational efficiency, providing interesting choices for simulating the infrared spectra of fullerene-related species. To facilitate the potential search, analysis, and interpretation of these fullerene-related species, like metallofullerenes, in space, they summarized all the scaled harmonic frequencies (see Table 4 in ref. 71). However, the conclusive identification of specific species in space remains challenging due to the potential coincidence of band features from different species or their concealment within the broad emission plateaus. Nevertheless, the work of Xu *et al.* provides a useful quantum-chemical procedure to model the band features of fullerene-related species, which could be used, in combination with astrophysical models, to potentially identify the presence of metallofullerenes in space.

4.3. Challenges in near-IR and UV-Vis simulations

Clearly, the detection of metallofullerenes not only relies on the simulation of their mid-IR transition, as discussed so far, but also on other spectral regimes like near-IR and UV-Vis, which include electronic transitions that could be affected by some internal chemical process like charge transfer from the metal to C_{60} cage. However, near-IR and UV-Vis simulations of endohedral fullerene species have proven to be computationally demanding and are not straightforward.[72–74] The description of quantum dynamics processes between the light and the molecules encapsulated inside the C_{60} becomes one of the initial challenges that should be tackled in order to go further in the accurate near-IR and UV-Vis simulations. These quantum dynamic effects have been accurately described in the translation-rotational scheme, which combined with experimental data, allowing the description of the inelastic neutron scattering spectra of small molecules inside the C_{60} carbon cage.[75] Ideally, similar quantum dynamic effects should be also included in the description of electronic transitions, which can improve the simulation of near-IR and UV-Vis spectra. However, these quantum dynamic effects imply the inclusion of more states in order to describe all the processes affecting

Table 2 Scaling factors obtained for several different functionals with the 6-31G** basis set. Extracted from ref. 71

Functionals (HF%)	Scaling factors		RMSE	Med. error	Time[a] (s)
BP86 (GGA)	1.0212 for <700 cm^{-1}	0.9941 for >700 cm^{-1}	10.2	5.3	1351
BPW91 (GGA)	1.0165 for <700 cm^{-1}	0.9905 for >700 cm^{-1}	10.7	5.5	1354
TPSSh (10%)	0.9972 for <700 cm^{-1}	0.9701 for >750 cm^{-1}	10.1	6.3	3321
B3LYP (20%)	0.9807 for <750 cm^{-1}	0.9697 for >750 cm^{-1}	11.0	5.2	3189
PBE0 (25%)	0.9755 for <750 cm^{-1}	0.9472 for >750 cm^{-1}	9.6	6.3	3390
M06 (27%)	0.9833 for <750 cm^{-1}	0.9519 for >750 cm^{-1}	10.6	7.0	4184
M06-2X (54%)	0.9631 for <1250 cm^{-1}	0.9485 for >1250 cm^{-1}	16.4	8.3	3702
ωB97XD	0.9635 for <750 cm^{-1}	0.9475 for >750 cm^{-1}	16.8	8.5	4407

[a] Time is evaluated by the frequency analysis of C_{60} on a 52-core SE24HIJTP workstation.

electronic transitions (*e.g.* spin–orbit coupling), making them unfeasible with current computational implementation. In contrast, the state-of-the-art time dependent DFT (TDDFT) stands as one of the main tools to perform UV-Vis simulation, however, its results depend on the method used to describe the nuclei-electron interaction (exchange–correlation). Thus, depending on the exchange–correlation selected, the electronic transition energies (wavelength) may vary considerably, particularly, in those systems where charge transfer and charge reordering affect the UV-Vis spectra as in the case of metallofullerenes.[76,77] As for near-IR spectroscopy, simulations in this case require a pure and full-anharmonic description of the vibrational states beyond the fundamental transition. Using Generalized 2nd-order vibrational perturbation theory (GVPT2), it is possible to obtain the near-IR spectra but at the expense of significant computational time.[78] Recent methods have been developed to overcome this limitation by using combined quantum mechanics with molecular mechanics (QM/MM) within GVPT2, but the current performance is limited to $\sim$30 atoms.[73] The link between near-IR and UV-Vis spectroscopies with the possible contribution of metallofullerenes to the DIBs, similar as C_{60}^{+}, could become the future driving force to move forward these limitations and achieve a more accurate modelling of the spectral fingerprint of these species under the astrophysical conditions.

5. Conclusions

We have reviewed the state-of-the-art advances towards the detection of metallofullerenes in space, tracking different astrophysical phenomena hinting their presence. The fundamental aspects of the spectral fingerpints of metallofullerenes, particularly in the mid-infrared region, have been presented to illustrate the uniqueness of these fullerene-related species. Laboratory methods described in this perspective show that metallofullerenes containing the most cosmically abundant metals can be synthesized, establishing the ground-base for their possible formation in space. Both experimental and theoretical calculations suggest that metallofullerenes, if confirmed to exist in space, could possibly contribute to the four features previously attributed to neutral C_{60}. We showed the implications of metallofullerenes in space in explaining the large infrared emission band ratios of C_{60} in different fullerene-rich circumstellar envelopes and in their potential contribution to DIBs. Furthermore, we highlight that metallofullerenes have several features beyond the mid- and near-infrared region, which may serve as an specific spectral region free of fullerenes for dectecting them in circumstellar and interstellar environments. The challenge, thus, remains to pinpoint the features associated with the presence of metallofullerenes in space, something that could be achievable by JWST. The JWST has unprecedented spectral resolution and sensitivity in the 4.9–28.3 μm spectral range obtained by the Mid-Infrared Instrument (MIRI) on board, providing great opportunity for distinguishing these species. In addition, the JWST with its near infrared spectrogragh (NIRSpec) operating in the 0.6–5 μm region, extends the spectral capability beyond that achieved by its predecesor, the Spitzer telescope. It is expected that such in-depth knowledge about the distinctive infrared signatures of these large carbon species would undoubtedly contribute to our understanding of the organic inventory and carbon evolution in the universe.

Author contributions

Ransel Barzaga: conceptualisation, investigation, writing – original draft, and writing – review and editing. Gao-Lei Hou: conceptualisation, investigation, writing – original draft, and writing – review and editing.

Conflicts of interest

There are no conflicts to declare.

Acknowledgements

This work is supported by the National Natural Science Foundation of China (92261101 and 22273070) and the Innovation Capability Support Program of Shaanxi Province (2023-CX-TD-49). R. B. would like to acknowledge that this perspective is based on the work from COST Action NanoSpace, CA21126, supported by COST (European Cooperation in Science and Technology). In addition, R. B. acknowledges the support from the State Research Agency (AEI) of the Spanish Ministry of Science and Innovation (MINCINN) under grant PID2020-115758GB-I00/AEI/10.13039/501100011033. G.-L. H. acknowledges the support from the ''Young Talent Support Plan'' of Xian Jiaotong University, as well as the Fundamental Research Funds for Central Universities, China.

Notes and references

1 S. Kwok, *Astron. Astrophys. Rev.*, 2016, **24**, 8.
2 B. A. McGuire, *Astrophys. J., Suppl. Ser.*, 2022, **259**, 30.
3 J. Cami, J. Bernard-Salas, E. Peeters and S. E. Malek, *Science*, 2010, **329**, 1180–1182.
4 D. Garca-Hernández, A. Manchado, P. Garca-Lario, L. Stanghellini, E. Villaver, R. Shaw, R. Szczerba and J. Perea-Calderón, *Astrophys. J., Lett.*, 2010, **724**, L39.
5 D. A. Garca-Hernández, N. K. Rao and D. L. Lambert, *Astrophys. J.*, 2011, **729**, 126.
6 P. Woods, *Nat. Astron.*, 2020, **4**, 299–305.
7 E. K. Campbell, M. Holz, D. Gerlich and J. P. Maier, *Nature*, 2015, **523**, 322–323.
8 A. Omont, *Astron. Astrophys.*, 2016, **590**, A52.
9 H. Fan, L. Hobbs, J. A. Dahlstrom, D. E. Welty, D. G. York, B. Rachford, T. P. Snow, P. Sonnentrucker, N. Baskes and G. Zhao, *Astrophys. J.*, 2019, **878**, 151.
10 S. Kwok, *Astrophys. Space Sci.*, 2022, **367**, 16.

11 J. Cernicharo, C. Cabezas, J. Pardo, M. Agúndez, O. Roncero, B. Tercero, N. Marcelino, M. Guélin, Y. Endo and P. de Vicente, *Astron. Astrophys.*, 2023, **672**, L13.
12 S. Barik, A. K. Kanakati, S. Dutta, N. R. Behera, R. K. Kushawaha and G. Aravind, *Astrophys. J.*, 2022, **931**, 47.
13 T. Trabelsi, V. J. Esposito and J. S. Francisco, *Astrophys. J.*, 2023, **949**, 55.
14 J. Highberger, C. Savage, J. Bieging and L. Ziurys, *Astrophys. J.*, 2001, **562**, 790.
15 L. M. Ziurys, *Proc. Natl. Acad. Sci. U. S. A.*, 2006, **103**, 12274–12279.
16 A. I. Karakas, *Mon. Not. R. Astron. Soc.*, 2010, **403**, 1413–1425.
17 A. I. Karakas, M. Lugaro, M. Carlos, B. Cseh, D. Kamath and D. A. García-Hernández, *Mon. Not. R. Astron. Soc.*, 2018, **477**, 421–437.
18 R. Barzaga, D. Garca-Hernández, S. Daz-Tendero, S. Sadjadi, A. Manchado and M. Alcami, *Astrophys. J.*, 2023, **942**, 5.
19 G.-L. Hou, O. V. Lushchikova, J. M. Bakker, P. Lievens, L. Decin and E. Janssens, *Astrophys. J.*, 2023, **952**, 13.
20 H. W. Kroto, J. R. Heath, S. C. Obrien, R. F. Curl and R. E. Smalley, *Nature*, 1985, **318**, 162–163.
21 H. Kroto, *Science*, 1988, **242**, 1139–1145.
22 J. R. Heath, S. C. O'Brien, Q. Zhang, Y. Liu, R. F. Curl, F. K. Tittel and R. E. Smalley, *J. Am. Chem. Soc.*, 1985, **107**, 7779–7780.
23 F. D. Weiss, J. L. Elkind, S. C. O'Brien, R. F. Curl and R. E. Smalley, *J. Am. Chem. Soc.*, 1988, **110**, 4464–4465.
24 Y. Huang and B. S. Freiser, *J. Am. Chem. Soc.*, 1991, **113**, 9418–9419.
25 H. W. Kroto and M. Jura, *Astron. Astrophys.*, 1992, **263**, 275–280.
26 J. Goebel and S. Moseley, *Astrophys. J., Part 2*, 1985, **290**, L35–L39.
27 H. P. Gail and E. Sedlmayr, *Astron. Astrophys.*, 1986, **166**, 225–236.
28 H. Campins and E. V. Ryan, *Astrophys. J., Part 1*, 1989, **341**, 1059–1066.
29 V. V. P. Perelygin, S. G. Stetsenko, N. T. Kashukeev and R. I. Petrova, *Bulg. J. Phys.*, 1990, **17**, 12–17.
30 J. Dorschner, J. Gürtler, T. H. Henning and H. Wagner, *Astron. Nachr.*, 1989, **310**, 303–309.
31 A. P. Jones, W. W. Duley and D. A. Williams, *Mon. Not. R. Astron. Soc.*, 1987, **229**, 213–221.
32 A. P. Jones and D. A. Williams, *Mon. Not. R. Astron. Soc.*, 1987, **224**, 473–479.
33 D. A. Garca-Hernández, S. Iglesias-Groth, J. A. Acosta-Pulido, A. Manchado, P. Garca-Lario, L. Stanghellini, E. Villaver, R. A. Shaw and F. Cataldo, *Astrophys. J. Lett.*, 2011, **737**, L30.
34 D. A. Garca-Hernández, E. Villaver, P. Garca-Lario, J. A. Acosta-Pulido, A. Manchado, L. Stanghellini, R. A. Shaw and F. Cataldo, *Astrophys. J.*, 2012, **760**, 107.
35 C. Gielen, J. Cami, J. Bouwman, E. Peeters and M. Min, *Astron. Astrophys.*, 2011, **536**, A54.
36 H. Hirashita and N. V. Voshchinnikov, *Mon. Not. R. Astron. Soc.*, 2013, **437**, 1636–1645.
37 E. Dwek, *Astrophys. J.*, 2016, **825**, 136.
38 P. W. Dunk, J.-J. Adjizian, N. K. Kaiser, J. P. Quinn, G. T. Blakney, C. P. Ewels, A. G. Marshall and H. W. Kroto, *Proc. Natl. Acad. Sci. U. S. A.*, 2013, **110**, 18081–18086.
39 P. W. Dunk, N. K. Kaiser, C. L. Hendrickson, J. P. Quinn, C. P. Ewels, Y. Nakanishi, Y. Sasaki, H. Shinohara, A. G. Marshall and H. W. Kroto, *Nat. Commun.*, 2012, **3**, 855.
40 P. W. Dunk, N. K. Kaiser, M. Mulet-Gas, A. Rodríguez-Fortea, J. M. Poblet, H. Shinohara, C. L. Hendrickson, A. G. Marshall and H. W. Kroto, *J. Am. Chem. Soc.*, 2012, **134**, 9380–9389.
41 P. W. Dunk, M. Mulet-Gas, Y. Nakanishi, N. K. Kaiser, A. Rodrguez-Fortea, H. Shinohara, J. M. Poblet, A. G. Marshall and H. W. Kroto, *Nat. Commun.*, 2014, **5**, 5844.
42 D. A. García-Hernández, A. Manchado and F. Cataldo, *Fullerenes, Nanotubes Carbon Nanostruct.*, 2020, **28**, 474–479.
43 H. Shinohara and N. Tagmatarchis, *Endohedral metallofullerenes: Fullerenes with metal inside*, John Wiley & Sons, 2015.
44 X. Lu, L. Echegoyen, A. L. Balch, S. Nagase and T. Akasaka, *Endohedral Metallofullerenes: Basics and Applications*, CRC Press, 2014.
45 Y. Matsuo, H. Okada and H. Ueno, *Endohedral lithium-containing fullerenes: preparation, derivatization, and application*, Springer, 2017.
46 S. Iglesias-Groth, F. Cataldo and A. Manchado, *Mon. Not. R. Astron. Soc.*, 2011, **413**, 213–222.
47 S. Iglesias-Groth, D. A. García-Hernández, F. Cataldo and A. Manchado, *Mon. Not. R. Astron. Soc.*, 2012, **423**, 2868–2878.
48 T. Jovanović, Đ. Koruga and B. Jovančićević, *et al.*, *J. Nanomater.*, 2017, 4360746.
49 D. A. Garcia-Hernandez, F. Cataldo and A. Manchado, *Fullerenes, Nanotubes Carbon Nanostruct.*, 2019, **27**, 695–701.
50 F. Cataldo and S. Iglesias-Groth, *Fulleranes: the hydrogenated fullerenes*, Springer Science & Business Media, 2010, vol. 2.
51 J. Xu, J. M. Bakker, O. V. Lushchikova, P. Lievens, E. Janssens and G.-L. Hou, *J. Am. Chem. Soc.*, 2023, **145**, 22243–22251.
52 M. Li, T. Yang, J. M. Bakker, E. Janssens and G.-L. Hou, *Cell Rep. Phys. Sci.*, 2022, **3**, 100910.
53 E. German, G.-L. Hou, J. Vanbuel, J. M. Bakker, J. A. Alonso, E. Janssens and M. J. López, *Carbon*, 2022, **197**, 535–543.
54 F. Calvo, Y. Li, D. M. Kiawi, J. M. Bakker, P. Parneix and E. Janssens, *Phys. Chem. Chem. Phys.*, 2015, **17**, 25956–25967.
55 G.-L. Hou, T. Yang, M. Li, J. Vanbuel, O. V. Lushchikova, P. Ferrari, J. M. Bakker and E. Janssens, *Angew. Chem., Int. Ed.*, 2021, **60**, 27095–27101.
56 A. C. Brieva, R. Gredel, C. Jäger, F. Huisken and T. Henning, *Astrophys. J.*, 2016, **826**, 122.
57 Y. Zhang, S. Sadjadi, C.-H. Hsia and S. Kwok, *Astrophys. J.*, 2017, **845**, 76.
58 J. Bernard-Salas, J. Cami, E. Peeters, A. P. Jones, E. R. Micelotta and M. A. T. Groenewegen, *Astrophys. J.*, 2012, **757**, 41.
59 J. Krełowski, *Publ. Astron. Soc. Pac.*, 2018, **130**, 071001.
60 E. K. Campbell, J. Rademacher and S. M. M. Bana, *Crystals*, 2021, **11**, 1119.

61 E. K. Campbell, *Mol. Phys.*, 2020, **118**, e1797918.
62 E. K. Campbell, E. S. Reedy, J. Rademacher, R. J. Whitby and G. Hoffman, *Astrophys. J.*, 2020, **897**, 88.
63 F. Negri, S. Alom, R. J. Whitby, M. H. Levitt, J. Rademacher, E. S. Reedy and E. K. Campbell, *Mol. Phys.*, 2024, **122**, e2173507.
64 J. Cami, *Proc. Int. Astron. Union*, 2013, **9**, 370–374.
65 B. Kern, D. Strelnikov, P. Weis, A. Böttcher and M. M. Kappes, *J. Phys. Chem. A*, 2013, **117**, 8251–8255.
66 S. Sadjadi, Q. A. Parker, C.-H. Hsia and Y. Zhang, *Astrophys. J.*, 2022, **934**, 75.
67 D. Jones and H. M. Boffin, *Nat. Astron.*, 2017, **1**, 0117.
68 K. B. Kwitter and R. Henry, *Publ. Astron. Soc. Pac.*, 2022, **134**, 022001.
69 M. Otsuka, F. Kemper, J. Cami, E. Peeters and J. Bernard-Salas, *Mon. Not. R. Astron. Soc.*, 2014, **437**, 2577–2593.
70 R. Barzaga, D. A. García-Hernández, S. Díaz-Tendero, S. Sadjadi, A. Manchado, M. Alcami, M. A. Gómez-Muñoz and T. Huertas-Roldán, *Astrophys. J., Suppl. Ser.*, 2023, **269**, 26.
71 J. Xu, A. Li, X. Li and G.-L. Hou, *Mon. Not. R. Astron. Soc.*, 2023, **525**, 3061–3074.
72 T. Y. Nikolaienko and E. S. Kryachko, *Nanoscale Res. Lett.*, 2015, **10**, 1–9.
73 L. Barnes, B. Schindler, I. Compagnon and A.-R. Allouche, *J. Mol. Model.*, 2016, **22**, 1–13.
74 M. Yamada, Z. Slanina, N. Mizorogi, A. Muranaka, Y. Maeda, S. Nagase, T. Akasaka and N. Kobayashi, *Phys. Chem. Chem. Phys.*, 2013, **15**, 3593–3601.
75 Z. Bačić, *J. Chem. Phys.*, 2018, **149**, 100901.
76 A. K. Srivastava, A. Kumar and N. Misra, *Chem. Phys. Lett.*, 2017, **682**, 20–25.
77 I. González-Veloso, J. Rodríguez-Otero and E. M. Cabaleiro-Lago, *Phys. Chem. Chem. Phys.*, 2019, **21**, 16665–16675.
78 G. Mulas, C. Falvo, P. Cassam-Chenaï and C. Joblin, *J. Chem. Phys.*, 2018, **149**, 144102.